High-level arsenite removal from groundwater by zero-valent iron

Hsing-Lung Lien [a,*], Richard T. Wilkin [b]

[a] *Department of Civil and Environmental Engineering, National University of Kaohsiung,
700 Kaohsiung University Rd., Kaohsiung 811, Taiwan, ROC*
[b] *National Risk Management Research Laboratory, US Environmental Protection Agency,
Office of Research and Development, 919 Kerr Research Drive, Ada, OK 74820, USA*

Abstract

The objectives of this study were to conduct batch and column studies to (i) assess the effectiveness of zero-valent iron for arsenic remediation in groundwater, (ii) determine removal mechanisms of arsenic, and (iii) evaluate implications of these processes with regard to the stability of arsenic and long-term remedial performance of the permeable reactive barrier (PRB) technology. A high concentration arsenic solution ($50 \, mg \, l^{-1}$) was prepared by using sodium arsenite (arsenic (III)) to simulate groundwater at a heavily contaminated Superfund site in the USA. Batch studies indicate that the removal of arsenic is a two-step reaction with fast initial disappearance of arsenite followed by a slow subsequent removal process. Flow-through columns were conducted at a flow rate of $17 \, ml \, h^{-1}$ under reducing conditions for 6.6 mo. Kinetic analysis suggested that arsenic removal behaves as a zero-order reaction at high arsenic concentrations. Arsenic removal rate constants decreased with time and arsenic breakthrough was observed in the column study. Arsenic removal capacity of zero-valent iron was determined to be approximately $7.5 \, mg \, As/g \, Fe$. Carbonate green rust was identified from the analysis of surface precipitates; arsenite uptake by green rust may be a major mechanism responsible for arsenic remediation by zero-valent iron. Analysis of HCl-extractable arsenic from iron samples indicated that approximately 28% of arsenic was in the form of arsenate suggesting that a surface oxidation process was involved in the arsenic removal with zero-valent iron.
© 2004 Elsevier Ltd. All rights reserved.

Keywords: Arsenic; Zero-valent iron; Groundwater remediation; Permeable reactive barriers

1. Introduction

Contamination of groundwater resources by arsenic is a well-known environmental problem that can have severe human health implications. Arsenic is released from soil environments into groundwater through natural processes and as a consequence of anthropogenic activities. Elevated concentrations of arsenic from natural sources ($>50 \, \mu g \, l^{-1}$) have been widely documented, for example, in Argentina, Bangladesh, Chile, West Bengal, Mexico, Taiwan, and parts of the United States (US) (e.g., Mandal, 1997; Nickson et al., 1998; Welch et al., 1988; McArthur et al., 2001; Rahman et al.,

---

* Corresponding author. Tel.: +886 7591 9221; fax: +886 7591 9376.
E-mail address: lien.sam@nuk.edu.tw (H.-L. Lien).

2001; Nordstrom, 2002). In the US, arsenic is a common inorganic contaminant found at Superfund sites. For example, in 1996 arsenic contamination was found at 226 Superfund sites, compared to 460 with lead contamination, 306 with chromium contamination, 226 with zinc, 224 with cadmium, 201 with copper, and 154 with mercury (US EPA, 1997). Levels of arsenic in groundwater >1–$10 \, mg \, l^{-1}$ are not unusual at many Superfund sites in the US.

In groundwater and surface water environments, arsenic is present as As(V) (arsenate) in oxidizing environments, while As(III) (arsenite) is the predominant arsenic form in reducing environments (Ferguson and Gavis, 1972; Cherry et al., 1979; Cullen and Reimer, 1989; Korte and Fernando, 1991; Smedley and Kinniburgh, 2002). Arsenite is more toxic than arsenate and tends to be more mobile in the environment. Arsenic is classified as a Group A carcinogen by the United States Environmental Protection Agency. Consequently, there is a continuing need to develop and improve existing remedial technologies for the removal of arsenic from groundwater.

Permeable reactive barriers (PRBs) represent a tested environmental remedial technology for treatment of groundwater contaminated with a wide array of both organic and inorganic contaminants (e.g., Gillham and O'Hannesin, 1994; Blowes et al., 2000). One challenge facing the development of the PRB technology for remediation of arsenic contamination in groundwater is the identification and evaluation of reactive media that can be employed to provide a long-term sink for metals while at the same time maintain permeability and hydraulic connectivity between the contaminant plume and the reactive treatment zone. To date the most commonly employed reactive reagent in PRBs has been zerovalent iron (ZVI). ZVI has proven to be an effective material for removing multiple contaminants including halogenated organic solvents (O'Hannesin and Gillham, 1998; Puls et al., 1999; Vogan et al., 1999; Wilkin et al., 2003), heavy metals (e.g., Shokes and Möller, 1999), radionuclides (Morrison et al., 2002), and arsenic (e.g., Lackovic et al., 2000; Farrell et al., 2001; Su and Puls, 2001a,b; Melitas et al., 2002a,b; Nikolaidis et al., 2003).

The removal of arsenic by using ZVI has received increased attention because studies have shown that ZVI has a high arsenic removal capacity. Yet because arsenic removal mechanisms apparently involve adsorption and possibly co-precipitation, the performance of ZVI is ultimately limited by its initial removal capacity and any additional capacity that may come about after iron metal corrodes in water. Most previous studies were conducted at relatively low concentrations of arsenic (e.g., $\leqslant 1000 \, \mu g \, l^{-1}$). In this paper, we assess the effectiveness of ZVI for high-level arsenic remediation in groundwater, evaluate removal mechanisms of arsenic, and evaluate implications of these processes with regard to the

stability of arsenic and long-term remedial performance of the PRB technology.

2. Materials and methods

2.1. Materials

Peerless ZVI with a BET surface area of $2.53 \pm 0.44 \, m^2 \, g^{-1}$ was obtained from Peerless Metal Powders & Abrasive, Detroit, MI (8–50 mesh). Reagent grade sodium arsenite, sodium bicarbonate, magnesium chloride, calcium chloride, and potassium sulfate were purchased from J. T. Baker. Sodium sulfate (99+%) and fine-grained silica sand were purchased from Aldrich and Fisher, respectively. Deionized water was used for preparation of all reagent solutions.

2.2. Simulated groundwater

Simulated groundwater was prepared based on the composition of contaminated groundwater found at a Superfund site in the US located near Helena, Montana. Arsenic contamination at this site stems in part from over 100 years of smelting activities. The chemical makeup of the simulated groundwater is provided as follows (in mg per l of deionized water): K_2SO_4 (13), Na_2SO_4 (1284), $NaHCO_3$ (370), $CaCl_2 \cdot 2H_2O$ (233), $MgCl_2 \cdot 6H_2O$ (136), and $NaAsO_2$ (108). The simulated solution has an arsenic concentration of about $50 \, mg \, l^{-1}$, mainly as arsenite, and a high sulfate concentration ($\sim 900 \, mg \, l^{-1}$). After preparation of the solution, concentrated hydrochloric acid was added drop wise to adjust pH to 7.25 ± 0.25 and the solution was purged with deoxygenated nitrogen gas to minimize the content of dissolved oxygen. At least 2-h of nitrogen purging was conducted before the prepared solution was used in batch or column experiments. Removal of concentrations of dissolved oxygen to $<0.2 \, mg \, l^{-1}$ was verified by using rhodazine D colorimetric test kits (Chemetrics, K-7501). All batch and column experiments were conducted in an anaerobic glove box under a N_2:H_2 (95:5, v/v) atmosphere.

2.3. Batch tests

Batch tests utilized ZVI and were conducted in 45 ml glass vials. Each vial was loaded with 5 g of reactive media and filled with simulated groundwater. Water volumes were determined gravimetrically. Batch bottles were mixed on an orbital shaker (50 rpm) at room temperature ($22 \pm 1 \, °C$) for time periods up to 400 h. The batch vials were periodically sampled by passing sample aliquots through $0.2 \, \mu m$ syringe filters and acidifying with concentrated nitric acid. In control experiments, batch vials were filled with arsenic solution and either

no iron filings or silica sand alone. Control samples were collected and analyzed at time intervals of about 0, 75, and 350 h. In all cases control samples showed stable pH values and no loss of initial arsenic concentrations were observed.

2.4. Column experiments

Column tests were run in 2.5 cm inner diameter by 30 cm length glass columns with stainless steel sampling ports. The columns contained inlet, outlet, and three intra-column sampling ports at 7.5, 15, 22.5 cm from the influent end. The sampling ports were $10 \, cm \times 0.158 \, cm$ (i.d.) needles connected with a stopcock and attached to the column using Nylon bushings with a three-layer silicone rubber septum. The needle was placed into the center of the column.

Two column experiments with different contents of iron were conducted in this study. Column A was filled with 372 g of 100% ZVI (Peerless) while the packing material for the column B consisted of an approximately 50/50 (v/v) ZVI and sand (SiO_2) mixture. An equal bulk volume of iron and sand was loaded separately into glass beakers and weighed before used. A well-homogenized iron (186 g) and sand (155 g) mixture was funneled into the column in five increments to ensure that column B was packed homogeneously. The porosity (ε) for column A and B was determined to be 0.73 and 0.55, respectively.

The batch and column experiments were performed under controlled redox conditions in an anaerobic chamber. In the column experiments, the influent solution was pumped through the columns at rates of about $17 \, ml \, h^{-1}$ by using a HPLC pump so that linear seepage velocities were about $3 \, ft \, d^{-1}$. Volumetric flow rates were measured periodically throughout the experiment to ensure consistency. The columns were sampled at time intervals up to 4000 h (6.6 mo). Samples were collected from the three intra-column sampling ports and the outlet from column A while only outlet samples were collected from column B. Oxidation-reduction potential and pH were measured with an Orion pH/mV meter equipped with a combination redox electrode and a combination pH electrode, respectively. Measured ORP values were converted to Eh values by adding the difference between the measured ORP of the reference solution and the theoretical ORP of the reference solution.

2.5. Analytical methods

Concentrations of arsenic and Na, K, Ca, Mg, and Fe were determined using inductively coupled plasma - optical emission spectroscopy (ICP-OES; Perkin Elmer Optima 3300 DV). Samples for arsenic speciation were preserved with ultrapure hydrochloric acid

(pH < 2.0) and analyzed by IC-HG-AFS (Ion Chromatograph-Hydride Generation-Atomic Fluorescence Spectrometer; IC, DIONEX and HG-AFS, PSA Excalibur). Arsenite and arsenate were first separated by an ion chromatograph, then reacted to form arsine through a hydride generation apparatus, and finally detected by an atomic fluorescence spectrometer. Sulfate and chloride concentrations were determined using capillary electrophoresis (Waters Quanta 4000E). Analyses of duplicate and spiked samples indicated an analytical error of less than 5% for all parameters analyzed in the laboratory.

2.6. Solid phase characterization

Solid materials that formed during the batch tests were extracted and analyzed by X-ray diffraction (XRD) to determine the mineralogy of the iron corrosion products. XRD measurements were performed using an X-ray diffractometer MiniFlex (Rigaku Co.) at 30 kV and 15 mA. The instrument uses a copper target tube radiation ($CuK_{\alpha 1}$) to produce X-rays with a wavelength of 1.54056 Å. Samples were placed on a quartz plate and were scanned from 5° to 60° (2θ) at a rate of $0.5° \, 2\theta \, min^{-1}$. The composition of the corrosion products was determined by ICP-OES after microwave digestion in dilute nitric acid. Total inorganic carbon measurements on the precipitates were made with a UIC carbon coulometer system (Engleman et al., 1985). Precipitate samples were mixed with 5% perchloric acid and evolved carbon dioxide gas was carried to the coulometer cell where it is absorbed and coulometrically titrated. Iron samples were extracted with 1 M HCl to dissolve carbonate and hydroxide precipitates. Total arsenic and arsenic speciation in the extractant solutions were determined using the methods described above. Prior to acid extraction procedures, the iron grains were not exposed to air.

3. Results

3.1. Batch studies

Results of the batch experiments with respect to arsenic removal showed a fast initial disappearance of arsenic followed by a slow subsequent removal of arsenic. Concentrations of arsenic decreased by a factor of 10 times within the first 50 h of reaction. After 200 h of reaction, arsenic concentrations generally decreased to $<0.5 \, mg \, l^{-1}$ or about a 100 fold decrease in concentration. Solution pH increased to between 8.0 and 9.0 after about 400 h. Concentrations of dissolved iron initially increased to values as high as $6 \, mg \, l^{-1}$ and then iron was removed from solution gradually with time. The formation of a green-colored precipitate that correlated

with the reduction of iron (and arsenic) concentrations from solution was observed.

3.2. Column studies

The flow-through column packed with ZVI (column A) was designed to remove arsenic from simulated groundwater running at $400 \, ml \, d^{-1}$ for approximately 200 d (∼6.6 mo). Results of the removal of arsenic in the four-outlet, iron-packed column are shown in Fig. 1a. Fitted curves simulated by the CFITIM program are also presented. The CFITIM code, including analytical solutions for both infinite and finite columns, was used to analyze the observed column effluent data using analytical solutions of the one-dimensional, non-equilibrium, convection-dispersion transport equations (Van Genuchten, 1981). The figure shows that the CFITIM model gives a satisfactory prediction for the behavior of arsenic uptake. A quick breakthrough was observed

in the first sampling port where arsenic emerged after about 200 h of continuous flow and saturated the front part of the column within 1800 h. In contrast, the appearance of arsenic in the output was detected at about 1000 h and gradually approached 60% of saturation after 4000 h of continuous flow. The trend in Eh decreased across the column. The Eh value of influent water was about +80 mV and decreased to about $-417 \pm 50 \, mV$ at the outlet. The pH of influent water was maintained at 7.25 ± 0.25; the pH of the effluent was steady at 8.0–8.5.

The total amount of arsenic removal was calculated by integrating the upper areas of the breakthrough curves (Fig. 1a). In order to analyze the arsenic removal capacity throughout the column, the column was equally divided into four zones: I, II, III, and IV (from inlet to outlet). The total amount of arsenic removal prior to sampling ports 1, 2, 3, and the outlet was determined to be 728, 1455, 2063, and 2802 mg As, respectively. The arsenic removal capacity of iron in each reaction zone can be determined by dividing net amount of arsenic removal by the iron mass present in each zone. Accordingly, the arsenic removal capacity in zones I, II, III, and IV was 6.8, 8.9, 6.5, and 7.9 $(mg \, g^{-1})$, respectively. The overall arsenic removal capacity for the full column averaged about 7.5 $mg \, g^{-1}$. To better characterize the performance of the iron column at different sections, we converted to a pore volume basis (Fig. 1b). After normalizing to a pore volume basis, the breakthrough curves obtained from each sampling port tend to be convergent. This is in agreement with the above-mentioned results of arsenic removal capacity that indicates a consistent performance of the column.

A column packed with a 50/50 mixture of iron and sand (column B) was conducted to investigate the performance of sand–iron mixtures. Fig. 2 shows the results
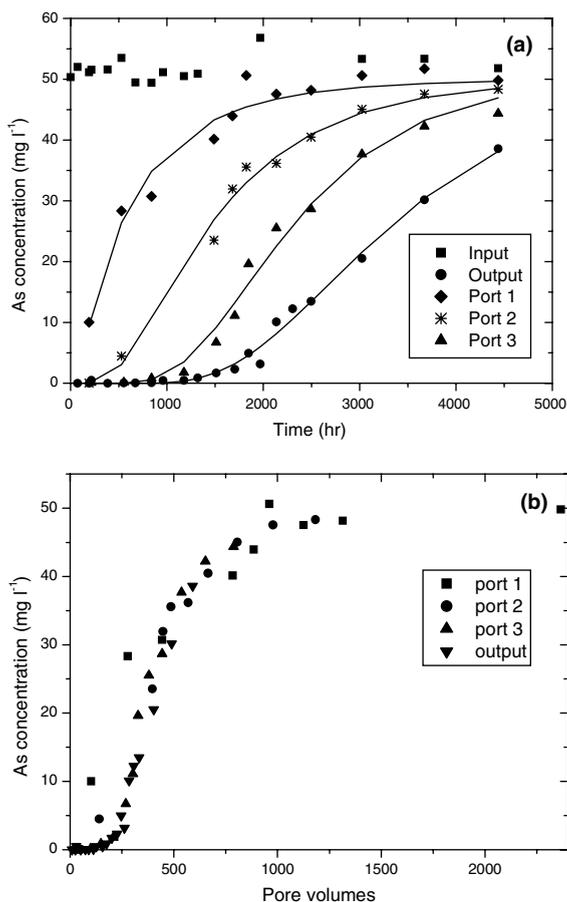

Fig. 1. Column experiment for the removal of arsenite by 100% zero-valent iron (a) concentration vs. time and (b) concentration vs. pore volume. The lines were derived from the CFITIM model.
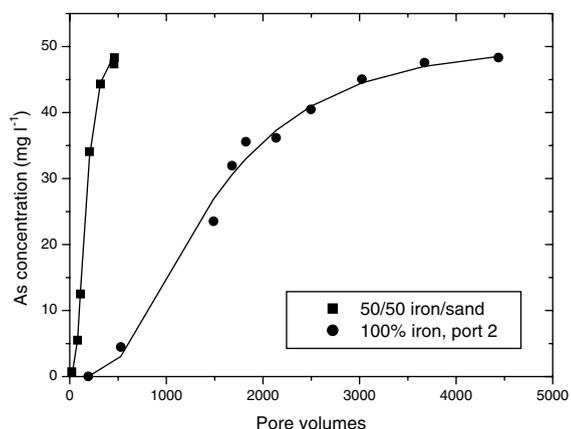

Fig. 2. Column experiment for the removal of arsenite by 50:50 iron and sand mixture. The lines were derived from the CFITIM model.

of arsenic removal using column B along with fitted curves. The amount of iron loaded in column B was approximately equivalent to the amount loaded into zones I and II in column A. For comparison, results of arsenic removal determined for sampling port 2 in column A are also incorporated in Fig. 2. The arsenic breakthrough is significantly faster than that observed from column A under similar flow conditions and input concentrations. The total amount of arsenic removal in column B was about 868 mg As. Because the batch study controls indicated that silica sand has no contribution to the arsenic removal, the arsenic removal capacity in column B can be attributed to the presence of iron and was found to be 4.7 mg As per g of iron. Clearly, the column packed with 100% iron (7.5 mg As/g Fe in average) had a better overall performance than that packed with the mixture of 50% iron and 50% sand. The results suggest that the use of iron for arsenic removal may not proceed under optimal conditions in column B, or in sand–iron mixtures. Because the size of silica sand is significantly smaller than that of ZVI particles used in the column experiments, dissolved arsenic may have directly passed through the column via "null" paths formed by the silica sand where arsenic did not react with iron. Consequently, the arsenic removal capacity determined in column B did not meet the saturated capacity.

4. Discussion

4.1. Kinetics

A combined zero- and first-order kinetic model (Eq. (1)) to describe arsenate removal by ZVI in batch tests has recently been proposed (Farrell et al., 2001):

$$\frac{d[As]}{dt} = \frac{-k_0[As]}{k_0/k_1 + [As]} \tag{1}$$

where [As] is the arsenate solution concentration, t is time, k_0 is the zero-order rate constant, and k_1 is the first-order rate constant. This equation indicates that arsenic removal follows first-order kinetics when [As] is sufficiently small and that zero-order kinetics are followed when [As] is significantly greater than k_0/k_1. Farrell et al. (2001) rationalized the mixed-order kinetic model by considering the competition between arsenic species and other dissolved solutes for reactive sites. At low concentrations, there is essentially no competition for sites, which results in first-order kinetics. At high arsenic concentrations, the number of reactive sites governs arsenic removal and uptake rates tend to be controlled by the availability of adsorption sites.

Analysis of the concentration data from this work was therefore conducted to determine both zero- and first-order rate constants for systems in which input arsenic was only present as arsenite. It might be expected that similar mechanisms will control arsenite and arsenate removal, but that overall rates might be different for these species (e.g., Lackovic et al., 2000; Su and Puls, 2001a). As mentioned above, batch tests indicated a two-step process for arsenite removal. Accordingly, the effects of arsenic concentration changes that are a consequence of uptake were taken into account (Table 1). At high arsenic concentrations (3.9–47 mg l^{-1}), a coefficient of determination (r^2) was 0.99 and 0.95 for first- and zero-order kinetics, respectively with respect to arsenic removal. Because both kinetic models can properly explain arsenic removal behavior using batch reactors, the determination of reaction orders requires further investigation. At low arsenic concentrations (0.2–3.9 mg l^{-1}), the coefficient of determination suggests that removal of arsenic follows a first-order reaction, which is consistent with the study of Farrell et al. (2001) (Table 1).

The observed first-order rate constant can be converted to a surface-area-normalized rate constant to provide a baseline comparison for studies conducted under different experimental conditions (Johnson et al., 1996).

$$k_{SA} = \frac{k_{obs}}{a_s \rho_i} \tag{2}$$

where k_{SA} is the surface-area-normalized rate constant (ml h^{-1} m^{-2}); k_{obs} is the observed first-order rate constant; a_s is the specific surface area of metal (m^2 g^{-1}); ρ_i is the mass concentration of iron (g ml^{-1}). At high arsenic concentrations, the k_{SA} was about 0.16 ml h^{-1} m^{-2}, which was about 3.7 times lower than a value (0.594 ml h^{-1} m^{-2}) determined from laboratory studies of ZVI and synthetic arsenic-containing solutions (Su and Puls, 2001a). Both studies were conducted under similar experimental conditions except a different mass concentration of iron was used. The metal concentration used in this study was four times higher than that used in the Su and Puls study. Therefore, the smaller value of k_{SA} determined in this study may be attributed to an excess of metal loaded. Normalization of observed rate constants by using Eq. (2) is based on an assumption that all the metals placed in batch reactors can completely react with reactants. However, k_{SA} values may be underestimated under conditions where an excess of metal is used in batch experiments. The excess of metal loading may lead to mass transfer resistance that causes an ineffective usage of metal reaction sites (Lien and Zhang, 1999).

Table 1
Arsenic removal rate constants estimated from the batch study

	Zero-order (mg l^{-1} h^{-1})	r^2	First-order (h^{-1})	r^2
High As(III)	0.841	0.947	0.048	0.993
Low As(III)	0.011	0.882	0.0088	0.944

Column studies were conducted to better characterize the reaction kinetics under continuous flow conditions. For the column experiments, residence time, t, was calculated by using Eq. (3):

$$t = \frac{\forall \times \varepsilon \times \chi}{Q \times L} \tag{3}$$

where $\forall$ is the empty column volume; ε is the porosity; χ is the distance along the column; Q is the flow rate; and L is the column length. Eq. (3) is based on an assumption that there is no dead volume in the column. The concentration profile of arsenic at different pore volumes in the column system was used to determine rate constants. Results of reaction kinetics analysis are shown in Table 2 obtained by fitting the experimental data from column tests with zero- and first-order kinetic models. The coefficient of determination suggests that the removal of arsenic at high concentrations exhibits zero-order kinetics from 580 to about 2490 h. This result supports the theory of competition between arsenic species for reactive sites proposed by Farrell et al. (2001). Also it would appear that similar kinetic models are followed regardless of whether input arsenic is as arsenate or arsenite, as input arsenic was only as As(III) in this study. Notice that kinetic analysis may not be accurate for data obtained below 190 h or above 3000 h because of insufficient data coverage. Below 190 h, removal of arsenic occurs immediately, because there are abundant reactive sites on the fresh material. After 3000 h, however, because most of the effective reactive sites have been saturated, arsenic uptake becomes a slow process. The dynamic process of arsenic uptake suggests that removal mechanisms involve sorption and precipitation so that removal rates and capacity are limited by the availability of reactive sorption sites and by the formation rate of iron corrosion products, i.e., new reactive sites.

4.2. As removal capacity

Unlike the As removal rate constant, the capacity of As removal appeared to be relatively constant at different reaction zones in column A. This implies that the As removal capacity should be a better design parameter than the As removal rate constant for the estimation of the amount of reactive material required for field-scale

Table 2
The coefficient of determination (r^2) for kinetic analysis from the column study

Residence time (h)	r^2 for zero-order kinetics	r^2 for first-order kinetics
<190	0.893	0.906
580–2490	0.999–0.968	0.926–0.856
2491–3672	0.930–0.934	0.855–0.895

Table 3
Comparison of arsenic removal capacity with different studies

	Capacity (mg g^{-1})	Reactors
This study	7.5[a,b]	Column
Lackovic et al. (2000)	1.15[c], 0.47[d]	Column
Su and Puls (2001a)	1.77[a]	Batch, Langmuir isotherm
Nikolaidis et al. (2003)	0.77[c,e]	Column

[a] Peerless iron.
[b] Based on the breakthrough occurring in column A.
[c] Connelly iron.
[d] Baker iron.
[e] Capacity was expressed as mg As per g of media containing both iron and sand.

applications of the PRB technology. Furthermore, compared with other similar studies, this study showed a comparatively high arsenic removal capacity (Table 3). It should be noted that the As removal capacity estimated by Lackovic et al. (2000) is based on the arsenic accumulation in the first 10 cm of their column experiment, not the saturated capacity of the column. They observed faster removal of both arsenite and arsenate near the inlet end of several columns packed with iron filings. A similar observation was also noted by Melitas et al. (2002a). They attributed the faster removal rate of arsenic near the column inlet to trace amounts of oxygen in the influent water that resulted in the increase of corrosion rate and an increase in the number of potential sorption sites.

4.3. Formation of surface precipitates

Fig. 3 shows the results of the X-ray diffraction analysis of the green precipitate that consistently formed in
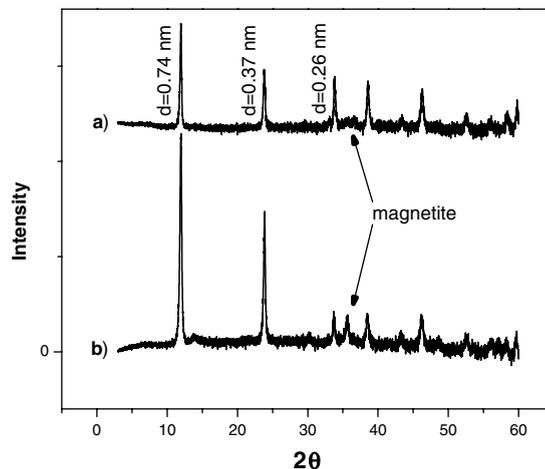
Fig. 3. X-ray diffraction scans of (a) a synthetic green rust and (b) a green precipitate from batch studies with ZVI.

the batch experiments. The pattern matches that of a synthetic carbonate green rust formed following a preparation recipe described in Bernal et al. (1959). Three predominant *d*-spacings at 0.74, 0.37, and 0.26 nm confirm the formation of carbonate green rust in the batch experiments. The concentration of inorganic carbon in the corrosion products was 1.26 ± 0.24 wt.% based on acid extraction and coulometric determination of the evolved CO_2. This carbon concentration is consistent with a carbonate green rust with composition $(Fe_4(II)$-$Fe_2(III)(OH)_{12}CO_3 \cdot xH_2O)$. Sulfate green rust was not identified although concentrations of sulfate in simulated water exceed 800 mg l^{-1} (molar $C/S \sim 0.5$). Digestion and analysis of the green rust precipitate indicated the presence of Fe (55 wt.%), Mg (0.6 wt.%), As (1.6 wt.%), and Si (0.6 wt.%). Consequently, arsenic uptake by green rust via adsorption or co-precipitation may be important mechanisms responsible for arsenic remediation by ZVI. In general, arsenic removal in zero-valent iron systems may involve many complicated processes (Table 4), however, the mechanism of arsenic removal by green rust is not certain at this point. Arsenic uptake could be related to adsorption of As(III) onto green rust or alternatively arsenite could replace carbonate in the interlayer position. The wt.% arsenic values determined by digestion are consistent with either or both of these possibilities. Randall et al. (2001) investigated the interaction between As(V) and sulfate green rust. They concluded that arsenic uptake was only by adsorption through the formation of inner-sphere surface complexes. The green rust, however, appears to be reacting to form magnetite and at this point it is unclear what happens to arsenic associated with green rust as transformation to magnetite proceeds.

A geochemical speciation and mass-transfer model (Geochemist's Workbench; Bethke, 1998) was used to evaluate reactions potentially controlling the concentrations of dissolved components in the effluent water. Saturations indices (SI), where $SI = \log(IAP/K)$, were calculated for the column effluent solutions using the measured cation and anion concentrations, pH, and Eh. The SI for carbonate green rust was calculated based upon the expression for the ion activity product (IAP) presented in Bourrié et al. (1999): $\log IAP = \log[Fe^{2+}] + 2pH - 1/3\log[e^-] + 1/6\log[CO_3^{2-}]$, with $\log K = 9.19$. In this expression $\log[e^-]$ is estimated using $-F\mathrm{Eh}/(2.303RT)$, where F is the Faraday constant, R is the molar gas constant, and T is temperature (K). Activity coefficients were calculated using the "B-dot" version of the extended Debye–Hückel equation. Geochemical calculations indicate that effluent water from column A was undersaturated with respect to gypsum, magnesite, and precipitated $Fe(OH)_2$, near-saturated with respect to aragonite and siderite, and slightly supersaturated with respect to the carbonate form of green rust (Fig. 4a). As noted above, carbonate green rust and

Table 4
Possible arsenic removal processes in zero-valent iron systems and examples

| Removal processes	Description	Examples	References
Surface adsorption	Immobilization of metals involves the binding of metal species onto the iron surface through, for example, surface complexation	Adsorption onto Fe^0 or Fe^0 corrosion products, e.g., iron (oxyhydr)oxides, to form bound arsenic such as inner-sphere, bidentate complexes	Lackovic et al. (2000), Manning et al. (2002), Melitas et al. (2002b) and Dixit and Hering (2003)
Precipitation	Nucleation and growth of a solid phase with repeating molecular unit in three dimensions	Symplesite $Fe_3(AsO_4)_2 \cdot 8H_2O$ Realgar As_4S_4	Nikolaidis et al. (2003)
Co-precipitation	Incorporation of element as a minor constituent in a mineral structure as it forms	Arsenic co-precipitation with: carbonate green rust $Fe_4(II)Fe_2(III)(OH)_{12}CO_3 \cdot xH_2O$ Ferrous sulfide/disulfide FeS, Fe_3S_4, or FeS_2	Nikolaidis et al. (2003) and This study
Redox reaction	Reduction	$As^{5+} + 2e^- \rightarrow As^{3+}$ (Insignificant) $As^{3+} + 3e^- \rightarrow As^0$ (Unlikely)	Farrell et al. (2001), Manning et al. (2002),
	Oxidation	$As^{3+} \xrightarrow{\text{oxidants}} As^{5+}$ (oxidants = e.g., carbonate green rust, maghemite, hematite)	Melitas et al. (2002b), Su and Puls (2004) and This study
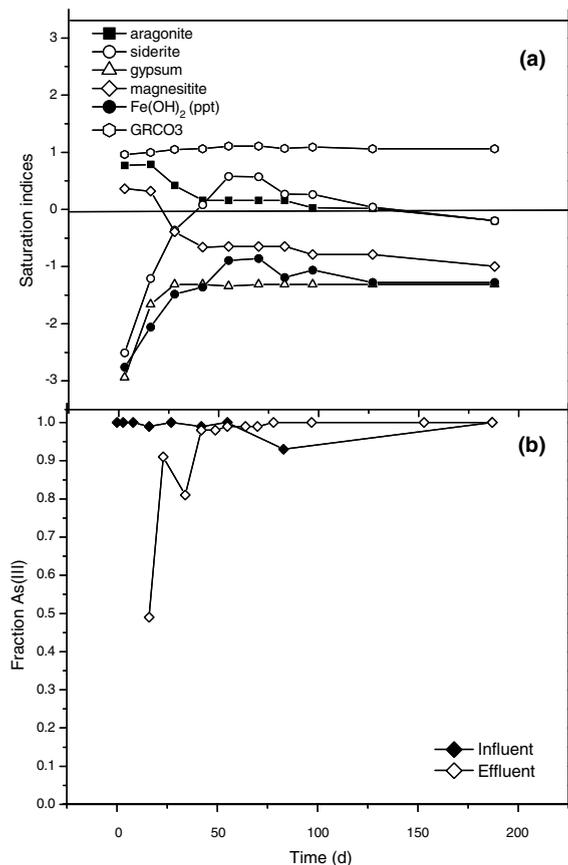
Fig. 4. (a) Saturation indices (SI) of selected minerals in effluent water from column A. GRCO3 represents carbonate green rust. (b) Arsenic oxidation state in influent and effluent water from column A.

Fig. 5. Arsenic extracted from iron grains (column A) and oxidation state of the extracted arsenic.

magnetite were the only minerals indicated by X-ray diffraction analysis. This observation and the constancy of the effluent SI with respect carbonate green rust suggests that green rust controlled the concentrations of Fe and carbonate; whereas, Eh and pH are likely governed by the rate of iron metal corrosion. Influent and effluent solutions were dominated by As(III) (Fig. 4b). The higher proportion of arsenate in the column effluent prior to 34 d suggests that some oxidizing potential was present initially that was subsequently consumed by reaction with arsenite.

Iron samples from column A were extracted in 1 N HCl at room temperature for 1 h. The supernatant was analyzed for total arsenic and arsenic speciation (Fig. 5). The recovery of the 1 N HCl leach was greatest near the inlet region of the column and progressively decreased towards the outlet region. Near the inlet region, the recovery of arsenic was approximately 80% of the total amount removed based upon integration of the breakthrough curves and the recovery near the outlet re-
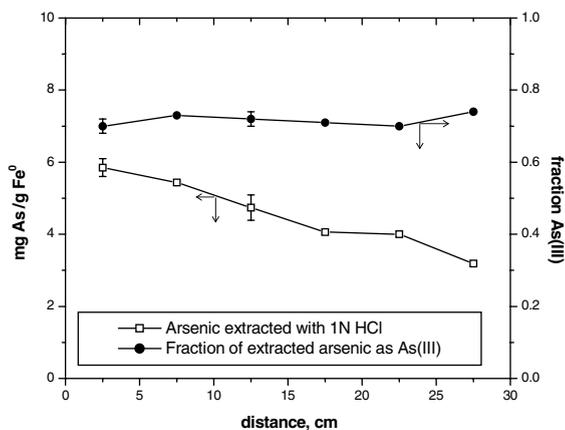
gion of the column was about 43%. This trend suggests that the conditions near the outlet region favor more stable arsenic removal, i.e., a greater proportion of arsenic is present in a form that is not extractable with 1 N HCl.

The oxidation state of arsenic in the extractable component is near-constant across the column with $72 \pm 2\%$ as As(III) and the remainder as As(V). Based on mass balance calculations we estimate that in order to account for the partial change in arsenic oxidation state from As(III) to As(V) via reaction with the most obvious oxidant, dissolved oxygen, a minimum influent dissolved oxygen concentration of $2.2 \, mg \, l^{-1}$ would have been necessary. Because the column experiment was conducted entirely in an anaerobic glove box with deoxygenated influent water, an oxidant other than oxygen is implicated. Su and Puls (2001a) also noted partial oxidation of As(III) to As(V) in batch experiments. Recent studies suggested that carbonate green rust may be responsible for the production of As(V) on the Fe^0 surfaces (Su and Puls, 2004). Input solutions to column A were always >95% in As(III). Output solutions after 34 d were similarly dominated by As(III) (Fig. 4b). The trends in the abundance of As(V) in the solid phase and in the effluent suggests that oxidation of As(III) in solution occurred early as arsenite solutions reacted with fresh iron surfaces and that arsenate production mainly occurred following arsenite sorption as a surface oxidation process.

5. Conclusions

The present investigation on the removal of arsenite (As(III)) with ZVI suggests that iron can be used as an effective remedial reagent for in situ remediation of groundwater contaminated with arsenic. As indicated by column studies at elevated levels of influent arsenic,

zero-order rate models better describe the arsenic removal behavior than do first-order rate models. According to the XRD analysis, arsenic uptake by green rust via adsorption or co-precipitation onto the iron surface may be important mechanisms, which reflect a finite arsenic removal capacity for ZVI. Consequently, the arsenic removal capacity should be a better parameter than the arsenic removal rate constant for the design of iron-based permeable reactive barriers. In addition, it was found that the arsenic removed near the outlet region was more stable than that near the inlet region based on acid extraction results. The abundance of arsenate (As(V)) observed in the solid phase suggested that an unusual surface oxidation process was involved in reducing conditions.

References

Bernal, J.D., Dasgupta, D.T., Mackay, A.L., 1959. The oxides and hydroxides of iron and their structural interrelationships. Clay Miner. Bull. 4, 15–30.

Bethke, C.M., 1998. The Geochemist's Workbench, Version 3.0. A Users Guide to Rxn, Act2, Tact, React, and Gtplot. The University of Illiniois.

Blowes, D.W., Ptacek, C.J., Benner, S.G., McRae, C.W.T., Bennet, T.A., Puls, R.W., 2000. Treatment of inorganic contaminants using permeable reactive barriers. J. Contam. Hydrol. 45, 123–137.

Bourrié, G., Trolard, F., Génin, J., Jaffrezic, A., Maître, V., Abdelmoula, M., 1999. Iron control by equilibria between hydroxy-Green Rusts and solutions in hydromorphic soils. Geochim. Cosmochim. Acta 63, 3417–3427.

Cherry, J.A., Shaikh, A.U., Tallman, D.E., Nicholson, R.V., 1979. Arsenic species as an indicator of redox conditions in groundwater. J. Hydrol. 43, 373–392.

Cullen, W.R., Reimer, K.J., 1989. Arsenic speciation in the environment. Chem. Rev. 89, 713–764.

Dixit, S., Hering, J.G., 2003. Comparison of arsenic (V) and arsenic (III) sorption onto iron oxide minerals: implications for arsenic mobility. Environ. Sci. Technol. 37, 4182–4189.

Engleman, E.E., Jackson, L.L., Norton, D.R., 1985. Determination of carbonate carbon in geological materials by coulometric titration. Chem. Geol. 53, 125–128.

Farrell, J., Wang, J., O'Day, P., Conklin, M., 2001. Electrochemical and spectroscopic study of arsenate removal from water using zero-valent iron media. Environ. Sci. Technol. 35, 2026–2032.

Ferguson, J.F., Gavis, J., 1972. A review of the arsenic cycle in natural waters. Water Res. 6, 1259–1274.

Gillham, R.W., O'Hannesin, S.F., 1994. Enhanced degradation of halogenated aliphatics by zero-valent iron. Ground Water 32, 958–967.

Johnson, T.L., Scherer, M.M., Tratnyek, P.G., 1996. Kinetics of halogenated organic compound degradation by iron metal. Environ. Sci. Technol. 30, 2634–2640.

Korte, N.E., Fernando, Q., 1991. A review of arsenic (III) in groundwater. Crit. Rev. Environ. Control 21, 1–39.

Lackovic, J.A., Nikolaidis, N.P., Dobbs, G.M., 2000. Inorganic arsenic removal by zero-valent iron. Environ. Eng. Sci. 17, 29–39.

Lien, H.-L., Zhang, W.-X., 1999. Dechlorination of chlorinated methanes in aqueous solutions using nanoscale bimetallic particles. J. Environ. Eng. 125, 1042–1047.

Mandal, B., 1997. Chronic arsenic toxicity in West Bengal. Curr. Sci. 72, 917–924.

Manning, B.A., Hunt, M.L., Amrhein, C., Yarmoff, J.A., 2002. Arsenic (III) and arsenic (V) reactions with zerovalent iron corrosion products. Environ. Sci. Technol. 36, 5455–5461.

McArthur, J.M., Ravenscroft, P., Safiulla, S., Thirlwall, M.F., 2001. Arsenic in groundwater: testing pollution mechanisms for sedimentary aquifers in Bangladesh. Water Resour. Res. 37, 109–117.

Melitas, N., Wang, J., Conklin, M., O'Day, P., Farrell, J., 2002a. Understanding soluble arsenate removal kinetics by zerovalent iron media. Environ. Sci. Technol. 36, 2074–2081.

Melitas, N., Conklin, M., Farrell, J., 2002b. Electrochemical study of arsenate and water reduction on iron media used for arsenic removal from potable water. Environ. Sci. Technol. 36, 3188–3193.

Morrison, S.J., Metzler, D.R., Dwyer, B.P., 2002. Removal of As, Mn, Mo, Se, U, V, and Zn from groundwater by zero-valent iron in a passive treatment cell: reaction progress modeling. J. Contam. Hydrol. 56, 99–116.

Nickson, R., McArthur, J., Burgess, W., Ahmed, K.M., Ravenscroft, P., Rahman, M., 1998. Arsenic poisoning of Bangladesh groundwater. Nature 395, 338.

Nikolaidis, N.P., Dobbs, G.M., Lackovic, J.A., 2003. Arsenic removal by zero-valent iron: field, laboratory and modeling studies. Water Res. 37, 1417–1425.

Nordstrom, D.K., 2002. Worldwide occurrences of arsenic in ground water. Science 296, 2143–2145.

O'Hannesin, S.F., Gillham, R.W., 1998. Long-term performance of an in situ "iron wall" for remediation of VOCs. Ground Water 36, 164–172.

Puls, R.W., Blowes, D.W., Gillham, R.W., 1999. Long-term performance monitoring for a permeable reactive barrier at the US Coast Guard Support Center, Elizabeth City, North Carolina. J. Hazard. Mater. 68, 109–124.

Rahman, M., Chowdhury, U., Mukherjee, S., Mandal, B., Paul, K., Lodh, D., Biswas, B., Chanda, C., Basu, G., Saha, K., Roy, S., Das, R., Palit, S., Quamruzzaman, Q., Chakraborti, D., 2001. Chronic arsenic toxicity in Bangladesh and West Bengal, India—a review and commentary. Toxicol. Clin. Toxicol. 39, 683.

Randall, S.R., Sherman, D.M., Ragnarsdottir, K.V., 2001. Sorption of As(V) on green rust $Fe_4(II)Fe_2(III)(OH)_{12}SO_4 \cdot 3H_2O)$ and lepidocrocite (γ-FeOOH): surface complexes from EXAFS spectroscopy. Geochim. Cosmochim. Acta 65, 1015–1023.

Shokes, T.E., Möller, G., 1999. Removal of dissolved heavy metals from acid rock drainage using iron metal. Environ. Sci. Technol. 33, 282–287.

Smedley, P.L., Kinniburgh, D.G., 2002. A review of the source, behavior and distribution of arsenic in natural waters. Appl. Geochem. 17, 517–568.

Su, C., Puls, R.W., 2001a. Arsenate and arsenite removal by zerovalent iron: kinetics, redox transformation, and implications for in situ groundwater remediation. Environ. Sci. Technol. 35, 1487–1492.

Su, C., Puls, R.W., 2001b. Arsenate and arsenite removal by zerovalent iron: effects of phosphate, silicate, carbonate, borate, sulfate, chromate, molybdate, and nitrate, relative to chloride. Environ. Sci. Technol. 35, 4562–4568.

Su, C., Puls, R.W., 2004. Significance of iron (II,III) hydroxycarbonate green rust in arsenic remediation using zerovalent iron in laboratory column test. Environ. Sci. Technol. 38, 5224–5231.

US EPA, 1997. Technology Alternatives for the Remediation of Soils Contaminated with As, Cd, Cr, Hg, and Pb. US Environmental Protection Agency, EPA/540/S-97/500.

Van Genuchten, M.T., 1981. CFITIM, US Salinity Laboratory, USDA-ARS, Riverside, CA.

Vogan, J.L., Focht, R.M., Clark, D.K., Graham, S.L., 1999. Performance evaluation of a permeable reactive barrier for remediation of dissolved chlorinated solvents in groundwater. J. Hazard. Mater. 68, 97–108.

Welch, A.H., Lico, M.S., Hughes, J.L., 1988. Arsenic in ground water of the western United States. Ground Water 26, 333–347.

Wilkin, R.T., Puls, R.W., Sewell, G.W., 2003. Long-term performance of permeable reactive barriers using zerovalent iron: geochemical and microbiological effects. Ground Water 41, 493–503.